

# PLASTIC STRAIN - CONCENTRATION FACTOR OF CYLINDRICAL BARS WITH CIRCUMFERENTIAL FLAT-BOTTOM GROOVE UNDER STATIC TENSION

<sup>1</sup>HITHAM M. TLILAN. <sup>2</sup>NASHMI H. ALRASHEEDI

<sup>1</sup>Department of Mechanical Engineering, Faculty of Engineering, The Hashemite University (HU), Zarqa 13115, Jordan.

<sup>2</sup>Department of Mechanical Engineering, Faculty of Engineering, Al Imam Mohammad Ibn Saud

Islamic University (IMISU), Riyadh 11432, Kingdom of Saudi Arabia,

E-mail: <sup>1</sup>hitham@hu.edu.jo, <sup>2</sup>nhrasheedi@imamu.edu.sa

**Abstract-** Geometrical irregularities affect stress and strain concentrations that are dominant and have been extensively studied in recent years. The existence of geometrical irregularities such as grooves is a common reason for failures. The elastic-plastic new Strain Concentration Factor (SNCF) for cylindrical bars with circumferential flat-bottom groove is studied here using the Finite Element Method (FEM). Specifically, the effect of flatness length on the strain concentration factor under elastic-plastic deformation and static tension is studied in this research. This new SNCF is defined under triaxial stress state. The employed specimens have constant gross diameter ( $D_0$ ) of 16.7 mm and net section diameter ( $d_0$ ) of 10.0 (mm). The flatness length ( $a_0$ ) is varied from 0.0~12.5 (mm) to study the influence of the flatness length on the new SNCF. Results showed that the elastic SNCF rapidly dropped from its maximum value at  $a_0 = 0.0$  (circumferential U – notch). The elastic SNCF reached a minimum value at  $a_0 = 3$  (mm) and remained constant beyond  $a_0 = 3$  (mm). At the groove root, the value of tensile load at yielding is increased as the flatness length increase, which indicates that the range of elastic deformation becomes larger with increasing flatness length. As the plastic deformation develops from the groove root; the SNCF increases from elastic deformation to maximum value. The rate of increase in the SNCF augments with increasing flatness length. The maximum value of the SNCF sharply decreases with increasing  $a_0$ . This maximum SNCF reaches its minimum at  $a_0 = 1$  (mm) then increases with increases with  $a_0$ . The maximum SNCF becomes nearly independent of  $a_0$  after  $a_0 = 4$  (mm). As a results; the severity of the notch vanishes as the flatness length enlarged.

**Keywords-** Groove, Notched bars, Strain concentration, Stress, Static tension.

## I. INTRODUCTION

Throughout industry, it is well known that notched machine elements such as bars, shafts and axels are subjected to a wide-range of severe mechanical loading types. The presence of those loading types gives a rise to stresses and strains in the components especially around notches and other irregularities. This is due to the development and application of fracture mechanics techniques which attempt to characterize a material by the consideration of the stress and strain relationships occurring at the tip of notches. Failure in elements is due to the development of stress or strain amplitude at the boundaries of those kinds of geometry. Therefore, at the vicinity of the geometrical irregularities the stress state is changed from biaxial to triaxial stress state immediately. As a result, failure occurred and localized at stress and strain concentrations region in machine elements and in design must be taken into consideration. To obtain Stress-Concentration Factor (SSCF) is common to use textbooks [1, 2]. Also, many studies have tackled this problem, such as a work initiated by Hardrath and Ohman, and Neuber [3,4].

A considerable amount of work has completed for common discontinuities or geometrical irregularities under static loading with regard to the determination of elastic SSCF. Results from experimental, theoretical solutions, and empirical formulae have presented in graphical representation [5 - 9]. Fewer

researchers have investigated and examined the SNCF for that type of geometry under static loading. Neuber (1961) has predicted the plastic SNCF increased and the plastic SSCF decreased from their elastic values as plastic deformation developed from the notch root under static tension [2]. In literature [8-13], these predictions have been confirmed experimentally or analytically. These outcomes indicated that for any type of loading, the SNCF is more important than the SSCF [14-20]. Because the plastic SNCF maintains a high value much greater than a unity, while the plastic SSCF decreases towards a unity. Most of these studies were for notches with an intermediate depth, and considered to give a strong notch effect.

A new SNCF has been defined under triaxial stress state and provided reasonable values consistent with the concave distributions of the axial strain at the net section. Additionally, this new definition has removed the contradiction in the conventional SNCF which has a value less than unity in spite of the concave distributions of the axial strain under elastic-plastic deformation. On the other hand, the conventional SNCF has defined under the uniaxial stress state and it is completely different from the stress state at the net section. Therefore, the SNCF must be defined under triaxial stress state at the net section [14-22] for any type of loading. Also, the new SNCF has made it possible for the first time to clarify the strain concentration in notches under creep. The purpose of this research is to improve and understand

the effect of flatness length ( $a_0$ ) on the new SNCF for circumferential grooves with flat bottom under static tension and elastic-plastic deformation. The FEM is used to obtain the stress and strain distributions. Also, The effect of groove flatness length  $a_0$  on the variations of the tensile load at yielding at the notch root ( $P_Y$ ) with deformation parameter  $2\ln(d_0/d)$  is investigated. The study covers deformation level close to the notch where the tensile strength occurs.

## II. STRAIN – CONCENTRATION FACTOR

Recently, a new Strain-Concentration Factor (SNCF) has defined for static tension [14-20]. The new SNCF is defined as the ratio of the maximum axial strain  $(\epsilon_z)_{\max}$  to the new average axial or the nominal strain at the net section  $(\epsilon_z)_{\text{av}}^{\text{new}}$ ;

$$K_\epsilon^{\text{new}} = \frac{(\epsilon_z)_{\max}}{(\epsilon_z)_{\text{av}}^{\text{new}}} \quad (1)$$

The new SNCF depends on the definition of the average axial strain because the maximum axial strain at the notch root is independent of definition. The axial strain assumed to be distributed uniformly at the net section when the notch effect is negligible. Therefore, the average axial or the nominal strain  $(\epsilon_z)_{\text{av}}^{\text{new}}$  for circumferentially notched cylindrical bars has been defined as follows

$$(\epsilon_z)_{\text{av}}^{\text{new}} = \frac{1}{\pi r_n^2} \int_0^{r_n} \epsilon_z(r) 2\pi r dr \quad (2)$$

where  $s = r/r_n$ . In the elastic deformation the  $(\epsilon_z)_{\text{av}}^{\text{new}}$  can be transformed into

$$\begin{aligned} (\epsilon_z)_{\text{av}}^{\text{new}} &= \frac{1}{\pi r_n^2} \int_0^{r_n} \left[ \frac{\sigma_z}{E} - \frac{\nu}{E} (\sigma_\theta + \sigma_r) \right] 2\pi r dr \\ &= \frac{(\sigma_z)_{\text{av}}}{E} - \frac{\nu}{E} \int_0^{r_n} (\sigma_\theta(s) + \sigma_r(s)) s ds \end{aligned} \quad (3)$$

where  $E$  is the Young's modulus,  $\nu$  is the Poisson's ratio and  $P$  is the tensile load. Equation (3) can be rewritten as

$$(\epsilon_z)_{\text{av}}^{\text{new}} = \frac{(\sigma_z)_{\text{av}}}{E} - \frac{2\nu}{E} \int_0^1 \{ \sigma_\theta(s) + \sigma_r(s) \} s ds \quad (4)$$

The  $(\epsilon_z)_{\text{av}}^{\text{new}}$  is defined under the triaxial stress state in the plastic deformed area at the net section as shown in Equation (4). Therefore, the plastic component of the axial strain is directly related to the triaxial stress state as presented by the theory of plasticity. At any deformation level, the definition under the triaxial stress state gives a reasonable consistency of SNCF with the concave distribution of the axial strain [14-20].

## III. MATERIALS AND GEOMETRIES

An Austenitic stainless steel and a Ni-Cr-Mo steel are investigated in this research. The materials properties and the polynomial coefficients are summarized in Table 1. The true stress strain curve has been obtained from the conventional tension using Universal testing machine. The experimental results

have been fitted with 5th degree polynomial as illustrated in Fig. 1. Figure 2 shows a cylindrical bar with circumferential flat-bottom notches and is used in the current study. Two different fillet radii 0.5 (mm) and 1.0 (mm) are used. The gross and net-section diameters are 16.7 (mm) and 10.0 (mm) to give a net-to-gross diameter ratio of 0.6. To study the effect of flatness length on the new SNCF, the gage length  $l_0$  is fixed to be 50 (mm) and flatness length  $a_0$  is varied from 0.0 to 12.5 (mm). It should be noted that  $a_0 = 0.0$  (mm) expressed the circumferentially U-notched cylindrical bars.

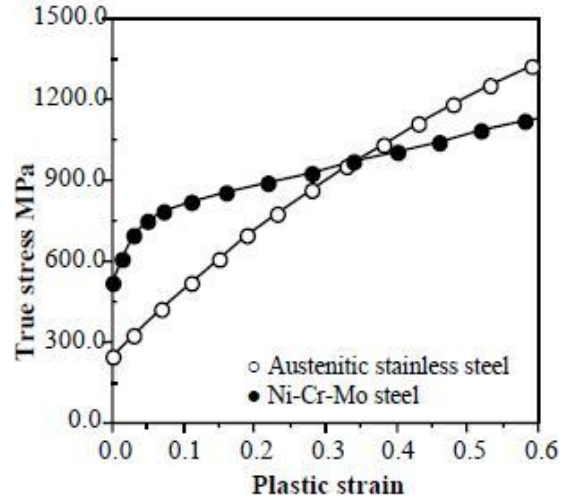


Fig. 1. True stress - plastic strain curve.

## IV. FINITE ELEMENT SIMULATIONS

The circumferential notched specimen modeled for this study is shown in Fig. 2. A quarter of the geometry was analyzed because of symmetry. A FE model was used for the employed specimen and constructed for tension in the Marc code using 8-nodes axisymmetric, isoperimetric quadrilateral ring element, with biquadratic interpolation and full integration type 28 in Marc classifications in this study. The mesh and the boundary conditions are presented in Fig. 3. The number of nodes was between 1717 and 15717 nodes, depending on the flatness length of the specimen. A mesh-sensitivity was conducted in this paper to examine the influence of mesh discretization on the numerical observations. The FEM calculations were performed under the axisymmetric deformation, which was applied at the end of the unnotched part.

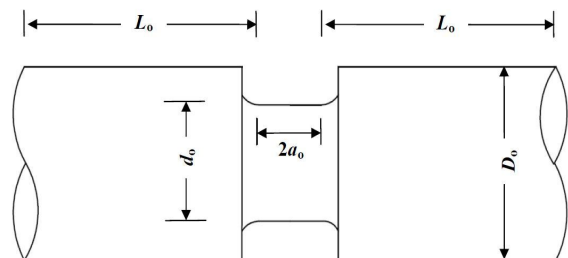


Fig. 2. Geometrical properties of the notched bar.

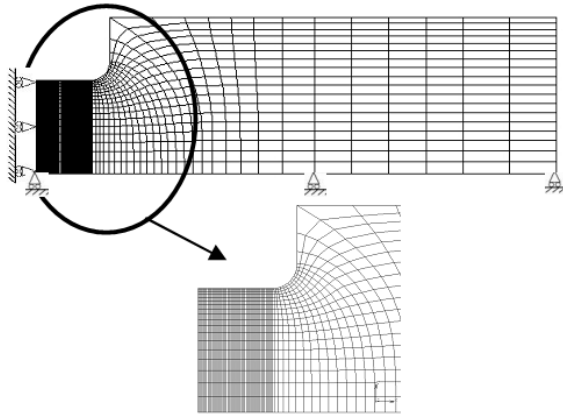


Fig.3. Finite element model and boundary condition.

## V. RESULTS AND DISCUSSIONS

### 5.1. Variation in tensile load with deformation

The tensile load ( $P$ ) is the greatest for the circumferential U-notch as shown in Fig. 4 for a specific value of  $2\ln(d_0/d)$ . Further, the tensile load decreases at the same value of  $2\ln(d_0/d)$  as the flatness length increases. Additionally, the tensile load values are nearly independent of  $a_0$  when  $a_0 \geq 3.0$  (mm) for the same level of deformation. For the same type of notches the study showed that the tensile loading of Ni-Cr-Mo steel is greater than that of an austenitic stainless steel. This occurs because of the flow stress of Ni-Cr-Mo steel is greater than of austenitic stainless steel [14-20]. Figure 4 also shows that as the flatness length increases the slope of tensile load .vs. deformation curve is reduced.

The values of the tensile loads at yielding at the notch root ( $P_Y$ ) are illustrated in Fig. 5. It is clearly indicated that the values of  $P_Y$  increases with increasing flatness length in the range  $0.0 \leq a_0 < 2.8$  (mm), while  $P_Y$  is independent of  $a_0$  in the range  $a_0 \geq 2.8$  (mm) [21]. The stress at the grooves root for  $a_0 < 2.8$  (mm) is greater than that of the grooves with  $a_0 > 2.8$  (mm) in the deformation range as shown in Fig. 4. It should be noted that the same results have been obtained for the effect of flatness length on tensile load  $P$  and tensile load at yielding ( $P_Y$ ) for radii 0.5 (mm).

### 5.2. Variation in the new SNCF with Tensile Load

The variations of the new SNCF with tensile load are plotted in Figures 6 and 7 for all fillet radii, groove flatness lengths and all material employed. The groove with zero flatness length is the circumferential U- notch (groove). As the tensile load increases, the initial response is elastic and the SNCF is constant in this level of deformation. An evident has been found that indicated the flatness length as well as the fillet radius has a prominent effect on the range of this constant value. Particularly, the flatness length effect on the range of elastic SNCF is more pronounced for  $0 \leq a_0 \leq 2.8$  (mm) than that for  $a_0 > 2.8$  (mm). Those results are also compatible with the reduction in the slope of elastic curve and with an increase in  $P_Y$  with

flatness length, as shown in Fig. 5. Therefore, the severity of the notch or groove is unnoticeable when the flatness length equal to 5 (mm). It also vanishes with increasing the notch or fillet radius [11-14]. This indicates that the elastic deformation capacity of the notched bars improved as the flatness length increases. The effect of the flatness length on elastic new SNCF for all specimens employed shows that the elastic SNCF in grooved specimens varies with flatness length in the ranges of  $a_0 \leq 3$  (mm) and independent of the flatness length in the range of  $a_0 > 3$  (mm). These results are true for all groove and fillet radii employed. However, the elastic SNCF of the circumferential U-groove ( $a_0 = 0.0$  (mm)) is greater than that of a groove with  $a_0 > 0.0$  (mm) [21].

As the plastic deformation develops from the notch and fillet root, the SNCF increases from its elastic value and reaches a peak value, as shown in Figures 6 and 7, respectively. The peak value becomes the maximum SNCF with increasing flatness length. In the range where  $a_0 > 3$  (mm) the new SNCF rapidly increases from its elastic value to its maximum as the plastic deformation develops from the notch or fillet root. The maximum SNCF sharply dropped from its value at  $a_0 = 0$  (mm) (i.e. Circumferential U - notch) when the flatness length increase for all notch radii employed, as shown in Fig. 8. The lowest value of the maximum SNCF occurs at flatness length of 1 and 2 (mm) for groove radii of 0.5 and 1 (mm), respectively. After that; the maximum SNCF increases with increasing flatness up to  $a_0 = 5$  (mm). In the range of  $a_0 > 5$  (mm) the maximum SNCF becomes nearly independent of the flatness length. This is an indication of the increases in the axial strain at the fillet root because of the localization and restriction of plastic deformation at the fillet root as the flatness length increased for  $0.0 < a_0 > 5$  (mm). This cannot be introduced by the conventional SNCF or the SSCF. Consequently, this is also due to the definition of the conventional SNCF under uniaxial stress state, which gives the SNCF values less than a unity with immediate development of the plastic deformation from the notch or fillet radius. Moreover, at the plastic deformation the SSCF becomes less than unity, which could not predict the current results.

## CONCLUSIONS

In the present work, the FEM is used to study the new elastic SNCF for circumferentially flat bottom notched bars in tension. From the current results, the following conclusions are justified:

1. For all groove radii and all flatness length employed; the strain-concentration factor increases with increasing deformation from its elastic to peak value as the plastic deformation develops from groove root. The rate of this increase in the SNCF becomes greater with increasing flatness length for all groove radii employed. Moreover, the peak value

becomes the maximum value as the flatness length increases. This is an indication that the existence of the flatness length reduces the severity of the notches or grooves. This true specifically in the range where  $0.0 < a_0 < 5$  (mm).

2. The maximum value of the SNCF rapidly decreases from its value for circumferentially U-notch; i.e.  $a_0 = 0.0$  (mm), and reaches its minimum at  $a_0 = 1$  (mm) for  $\rho_0 = 0.5$  (mm) and at  $a_0 = 2$  mm for  $\rho_0 = 0.5$  (mm). It is nearly independent of the flatness length for  $a_0 \geq 5.0$  (mm).

3. The SNCF values for any flatness length are less than that of the Circumferential U-notch at any level of deformation. This is an indication that the interference effect due to the flatness length reduce the severity of the notch interns of a reduction in the SNCF values.

4. The elastic SNCF rapidly decreases from its value at  $a_0 = 0.0$  (mm), i.e. circumferentially U-notch, to a minimum value at  $a_0 = 3.0$  (mm). For  $a_0 \geq 3.0$  (mm) the elastic SNCF is nearly independent of  $a_0$ . The range of elastic SNCF becomes lager with increasing  $a_0$  and increasing notch radius. It has been clarified that the elastic deformation capacity of the notched bars improves due to the presence of flatness length. This means that the values of tensile load at yielding at the notch root  $P_Y$  improves with increasing  $a_0$  up to 2.8 (mm). For larger  $a_0$ , the values of  $P_Y$  are nearly independent of  $a_0$  [21].

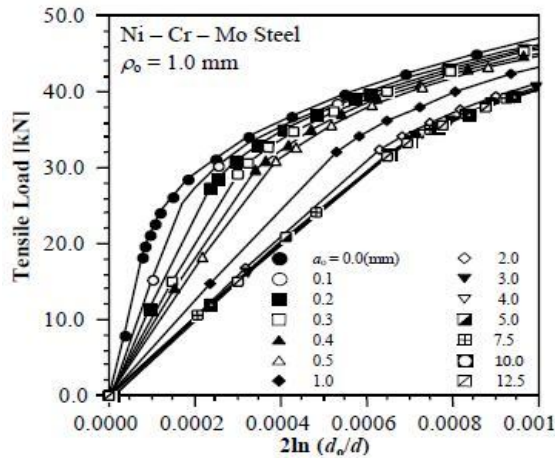


Fig.4. Effect of flatness length on variation of tensile load with deformation.

Table 1: Mechanical properties and polynomials coefficients

$\sigma_{me} = B_0 + B_1 \epsilon_p + B_2 \epsilon_p^2 + B_3 \epsilon_p^3 + B_4 \epsilon_p^4 + B_5 \epsilon_p^5$							
Material	Plastic strain range	$B_0$	$B_1$	$B_2$	$B_3$	$B_4$	$B_5$
Austenitic stainless steel 206.0, 0.30, 245.9	$\epsilon_p \leq 0.2$	$2.459 \times 10^2$	$4.389 \times 10^3$	$-3.265 \times 10^4$	$2.402 \times 10^5$	$-8.899 \times 10^5$	$1.258 \times 10^6$
	$0.2 < \epsilon_p \leq 0.5$	$3.789 \times 10^2$	$1.535 \times 10^3$	$1.173 \times 10^3$	$-1.874 \times 10^3$	0.0	0.0
	$\epsilon_p > 0.5$	$4.396 \times 10^2$	$1.865 \times 10^3$	$-7.617 \times 10^2$	$1.937 \times 10^2$	0.0	0.0
Ni-Cr-Mo steel 206.0, 0.30, 525.0	$\epsilon_p \leq 0.1$	$5.250 \times 10^2$	$7.644 \times 10^3$	$-7.377 \times 10^4$	$2.596 \times 10^5$	0.0	0.0
	$\epsilon_p > 0.1$	$7.426 \times 10^2$	$6.945 \times 10^2$	$-8.143 \times 10$	0.0	0.0	0.0

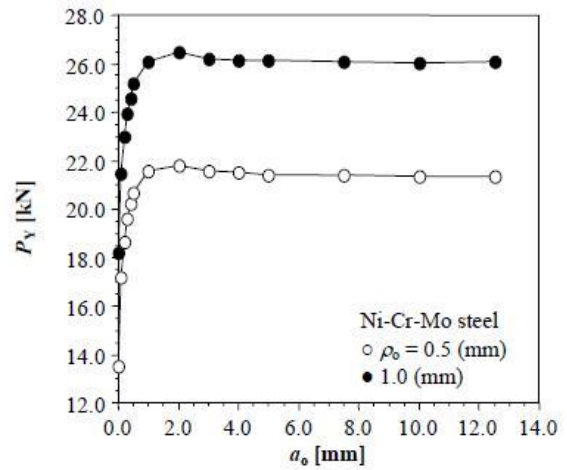


Fig. 5. Effect of flatness length on tensile load at yielding at the groove root.

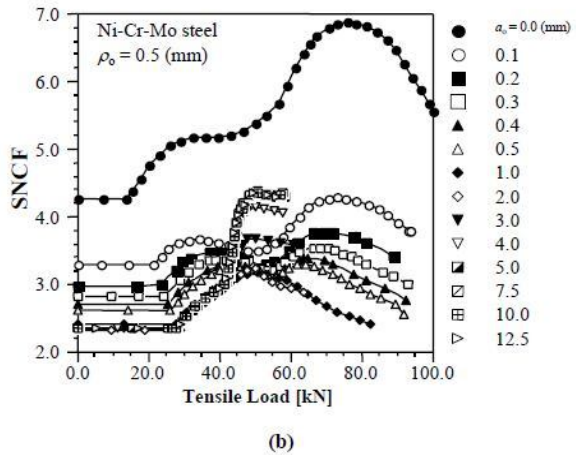
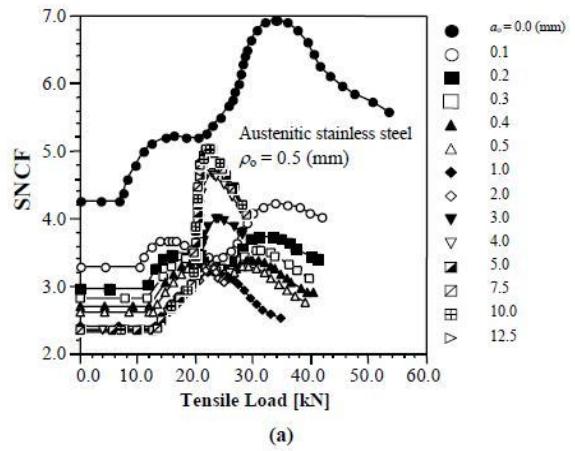


Fig.6. (a & b) Effect of flatness length on variations of SNCF with tensile load for 0.5 (mm) notch.

## REFERENC

- [1]. Nishida K. Stress concentration. (In Japanese). Tokyo: Morikita Shuppan; 1974.
- [2]. Pilkey W.D. Peterson's Stress Concentration Factors. New York: Wiley; 1997.
- [3]. H.F. Hardrath, L. Ohman, "A study of elastic and plastic stress concentration factors due to notches and fillets in flat plates". National Advisory Committee Aeronautics, NACA Report 1117, 1953.
- [4]. H. Neuber, "Theory of stress concentration factor for shear-strained prismatical bodies with arbitrary nonlinear



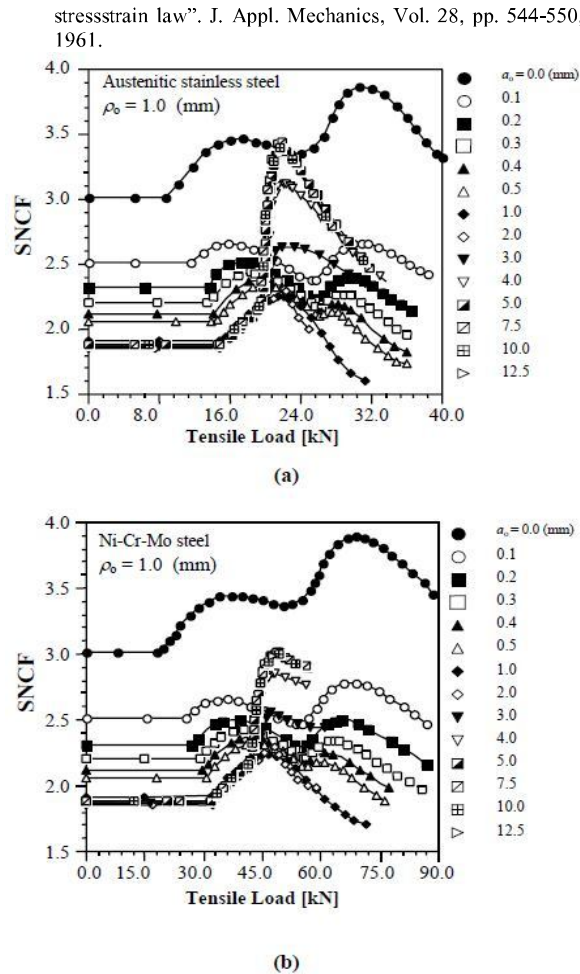


Fig. 7. (a & b) Effect of flatness length on variations of SNCF with tensile load for 1.0 (mm) notch.

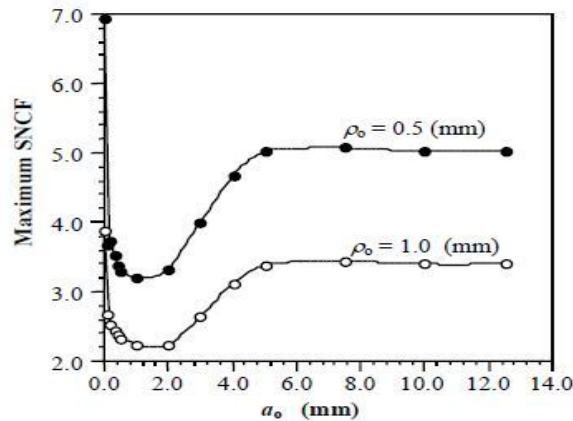


Fig. 8. Effect of flatness length on the maximum SNCF.

- [1]. M.M. Leven, M.M. Frocht, "Stress-concentration factors for single notch in flat bar in pure and central bending". J. Appl. Mechanics, Vol. 74, pp. 560-56, 1952.

- [2]. A. Kato, "Design equation for stress concentration factors of notched strips and grooved shafts". J. strain analysis, Vol 26, pp. 21-28, 1991.
- [3]. N.A. Noda, M. Sera, Y. Takase, "Stress concentration factors for round and flat test specimens with notches". Int. J. Fatigue, Vol. 17, no. 3, pp. 163-178, 1995.
- [4]. P.S. Theocaris, "Experimental solution of elastic-plastic plane stress problems". J. Appl. Mechanics, Vol. 29, pp. 735-743, 1962.
- [5]. P.S. Theocaris, E. Marketos, "Elastic-plastic strain and stress distribution in notched plates under plane stress". J. Mech. Phys. Solids, Vol. 11, pp. 411-428, 1963.
- [6]. A. J. Durelli, C.A. Sciammarella, "Elastoplastic stress and strain distribution in a finite plate with a circular hole subjected to unidimensional load". J. Appl. Mechanics, Vol. 30, pp. 115-121, 1963.
- [7]. P.S. Theocaris, "The effect of plasticity on the stress distribution of thin notched plates in tension". J. Franklin Inst., Vol. 279, pp. 22-38, 1965.
- [8]. K. Ogura, N. Miki, K. Ohji, "Finite element analysis of elastic-plastic stress and strain concentration factors under plane strain and axisymmetric conditions". (In Japanese). Trans. Japan Soc. Mech. Engrs., Vol. 47, pp. 55-62, 1981.
- [9]. S.J. Hardy, M.K. Pipelzadeh, "An assessment of the notch stress-strain conversion rules for short flat bars with projections subjected to axial and shear loading". J. Strain Analysis, Vol. 31, no. 2, pp. 91-110, 1996.
- [10]. T. Majima, "Strain-concentration factor of circumferentially notched cylindrical bars under static tension". J. Strain Analysis, Vol. 34, no. 5, pp. 347-360, 1999.
- [11]. H.M. Tlilan, N. Sakai, T. Majima, "Strain-concentration factor of a single-edge notch under pure bending. (In Japanese)". Yamanashi District Conference, no. 40-4, Japan, 2004.
- [12]. H.M. Tlilan, N. Sakai, T. Majima, "Strain-concentration factor of rectangular bars with a single-edge notch under pure bending, (In Japanese)". J. Soc. Mat. Science, Vol. 54, no. 7, pp. 724-729, 2005.
- [13]. H.M. Tlilan, S. Yousuke, T. Majima, "Effect of notch depth on strain-concentration factor of notched cylindrical bars under static tension". European Journal of Mechanics A / Solids, Vol. 24 no. 3, pp. 406-416, 2005.
- [14]. H.M. Tlilan, N. Sakai, T. Majima, "Effect of notch depth on strain-concentration factor of rectangular bars with a single-edge notch under pure bending". Int. J. Solids and Structures, Vol. 43, pp. 459-474, 2006.
- [15]. H. M. Tlilan, A. S. Al-Shyyab, T. Darabseh., T. Majima, "Strain-Concentration Factor of notched cylindrical Austenitic stainless Steel bar with double slant circumferential U- notches under static tension". Jordan J. Mech. Ind. Engg. Vol. 1, pp. 105-111, 2007.
- [16]. H.M. Tlilan, A.S. Al-Shyyab, A.M. Jawarneh, A.K. Ababneh, "Strain-concentration factor of circumferentially vnotched cylindrical bars under static tension". Journal of Mechanics, Vol. 24, no. 4, pp. 419-428, 2008.
- [17]. Hitham M. Tlilan, "Elastic Strain-Concentration Factor of Cylindrical Bars with Circumferential Flat-Bottom Groove under Static Tension", World Academy of Science, Engineering and Technology 76, Venice, Italy, April 2011.
- [18]. H.M. Tlilan, N.H. AlRasheedi, "Strain - concentration factor of notched bars under combined loading". International Review of Mechanical Engineering", Vol. 8, no. 4, pp. 791-797, 2014.

★★★